島根大学教育学部紀要（自然科学）第37巻　１頁～８頁　平成15年12月

# Mechanism of High Modulus in Zone-drawn Polyethylene Fibers

Tetsuya TAKAHASHI*

---

高橋　哲也

ゾーン延伸されたポリエチレン繊維の高弾性率化機構

---

## ABSTRACT

The structure of high modulus, high strength polyethylene (hereafter " PE ") fibers prepared by the continuous multi-stage zone-drawing method was studied primarily through examination of thermal shrinkage characteristics. Crystallinity dependence of the young's modulus exhibited a critical point of crystallinity where the dependency started to increase. Samples having high modulus, which is highly dependent on crystallinity, showed a thermal shrinkage initiating temperature, Ts, that was higher than that of a sample with less dependency and that was found to be higher than Tα.

The structure and mechanical properties of the samples after heat-treatment were also investigated to find that the young's modulus and amorphous birefringence stayed at high values, although with a little drop, when the heat treatment was made at 60℃, a temperature below Tα; whereas both values markedly dropped when the heat treatment was made at 80℃, a temperature above Tα. These findings indicate that thermal shrinkage took place after relaxation of crystallites, resulting in marked drops in the young's modulus and amorphous birefringence.

## 1. Introduction

Since the inventions1) that the growth method of fibrous crystals from a dilute solution of ultrahigh molecular weight PE (UHMWPE) and fibers obtained by ultra-drawing of gel-span fibers exhibited high-strength and high-modulus, studied on drawing properties and ultra-drawn structure of such gels have come to be actively conducted2)3). It has become clear that the long spacing structure, thought hitherto as a basic characteristic of flexible polymers, can diminish in some cases of strong drawing, shifting to an extended structure as of a rigid polymers.

On the other hand, processes to produce high-strength, high-modulus materials from medium molecular weight PE can be exemplified by zone-drawing4)−7), die-drawing, and high pressure extrusion. In the plastic deformation process accompanied by necking, folded molecular chains or lamellae are effectively unfolded at the neck to construct crystallite blocks as the result of microfibril structure formation. Zone-drawing is a process to utilize positively this phenomenon through application of heat and a drawing stress.

The authors previously reported8)−11) that continuous zone-drawing of medium molecular weight PE could produce continuously PE filaments with the modulus of 74Gpa, attaining 80GPa by its multi-stage version. In the present study, the mechanism of high modulus development in zone-drawn fibers was investigated from the aspect of the mechanism of crystallite block formation.

---

*Department of Home Economics Education, Shimane University, Matsue, Japan

## 2. Experimental

### 2.1 Samples

The high density PE " SHOLEX high-tenacity filament grade " ($MW=15\times10^4$, $Mw/Mn=3\text{-}4$) produced by SHOWA DENKO K.K., was melt-spun through an extruder to make the as-spun filaments, which had a diameter of about 0.7 mm. a density of 0.953, and a birefringence $\Delta n$ of $3.2\times10^{-3}$.

### 2.2 Drawing Process

The continuous multi-stage zone-drawing apparatus, the same as previously reported, was used, which consisted of a delivery roll and a take-up roll so as for the as-spun filament, feeded from the feed-roll, to be smoothly drawn with necking and further drawn in three stages without necking.

Under the conditions of the drawing temperature of 95-135°C and the feeding rate $V_c$ of 2-10 mm/min, fiber samples with four different draw ratios were prepared by the first-stage drawings with necking with varied take-up rates $V_d$. Fiber samples of multi-stage drawing were also prepared by conducting an additional three-stage drawing without necking after the first-stage drawing with necking.

#### a) Density

A density gradient tube of a water-methanol system was used. The density was measured after standing at 20°C for one day. The volume fraction crystallinity was calculated by using 1.00 and 0.852 g/cm$^3$ for densities of crystalline and amorphous phases, respectively.

#### b) Birefringence

The birefringence ($\Delta n$) of samples was measured by using a polarizing microscope equipped with a Na-D line light source (wave length of 589 μm) and a Berec compensator. The birefringence of amorphous molecular chain was calculated by using following equations:

$$\Delta n = \Delta n_c \cdot X_c + \Delta n_a \cdot (1-X_c) \quad \cdots\cdots\cdot \ (1)$$

$$\Delta n_c = \Delta n_c^* \cdot f_c \quad \cdots\cdots\cdot \ (2)$$

Where $\Delta n_c$ and $\Delta n_z$ denote birefringences of crystallite and amorphous phases, respectively. And $\Delta n_c^*$ denotes an ultimate birefringence of crystallite phase, being 0.057[12)], while $f_c$ means a crystalline orientation factor and Xc a volume fraction crystallinity. The morphological birefringence $\Delta n_{form}$ was generally very small and neglected.

#### c) Wide-Angle X-ray Diffraction

X-ray generator, a product of Rigaku Co. Ltd. was used with a Cu-Kα line and a Ni-filter. The diffraction intensity curve at an output of 40 kV and 150 mA was measured by using a scintillation counter. The orientation factor along the c-axis of the crystal was obtained by the angle dependence of X-ray diffraction intensity at the (200) reflection.

#### d) Mechanical properties

Dynamic modulus (E') was measured by use of VIBRON Model DDV-II, made by ORIENTECH Co., at the drive wave-number of 110 Hz and the temperature heating rate of 2°C/min and in the temperature range of -150°C to 120°C. Loss modulus (E") in the same temperature range was also measured to obtain α-relaxation temperature. The tensile strength was obtained by a stress at break by using a TENSILON UTM-III-500 type of ORIENTECH Co. in a room thermostated at 23°C using a sample of 50 mm in length and a strain rate of 100%/min.

#### e) Thermal contractile property

A sample fiber, cut into a length of 10 cm, was placed in a Oil-bath (using silicone oil) for 10 min, and then subjected to measurement of the fiber length by use of slide calipers. The thermal shrinkage was calculated as regard to the free length of the fiber.

## 3. Results and Discussion

### 3.1 Orientation behavior of amorphous molecular chains

Fig. 1 shows the drawing-condition dependence of the crystallinity. The higher the drawing temperature, the crystallinity was higher, becoming higher with an increase in draw ratio. The marks with a bar over them are of the multi-stage drawing samples, obtained by drawing with necking followed by a further three-stage drawing without necking, and are positioned on a extrapolating line for each drawing temperature.

Fibers prepared by continuous zone-drawing with a draw ratio over 10 show the orientation factor close to that of a perfect orientation; therefore, the birefringence of the amorphous phase was estimated by subtracting the contribution of the crystalline phase (nearly constant as 0.0579) from the observed birefringence. Fig. 2 shows the drawing-condition dependence of the amorphous birefringence. The birefringence of crystallite, taking a constant value, is expressed by a single broken line. The amorphous birefringence is found to depend much on both the drawing temperature and draw ratio. In particular, the amorphous birefringence of the sample multistage-drawn at a drawing temperature of 120°C and draw ratio of 25.3 attained the value as high as $104\times10^{-3}$ .

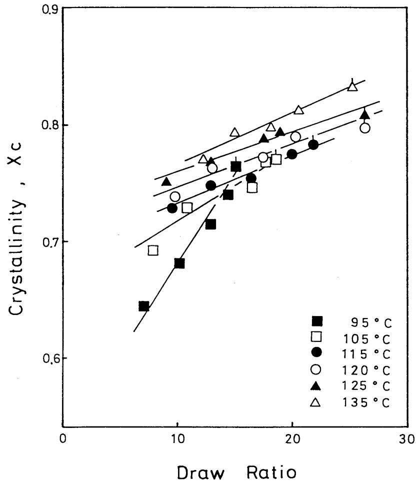

Fig. 1 Crystallinity versus draw ratio for different drawing temperature. The marks with a bar over them are of the multi-stage drawing samples.

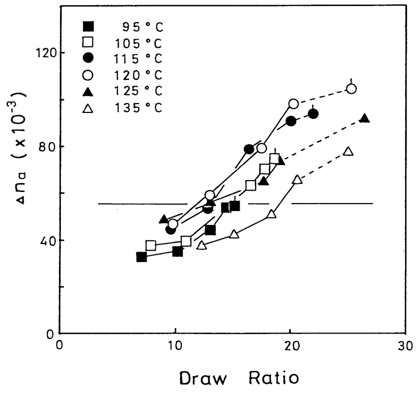

Fig. 2 Amorphous birefringence versus draw ratio for different drawing temperature. The marks with a bar over them are of the multi-stage drawing samples.

### 3.2 Mechanical properties

Fig. 3 shows the drawing temperature and draw ratio dependence of young's modulus. For all drawing temperatures, the modulus increased with an increase in draw ratio, the values for multi-stage drawn samples being positioned on an extrapolating line for each drawing temperature. For a given draw ratio, high modulus is obtained at the drawing temperature range of 115-120°C, which is considered the best condition in zone-drawing. This temperature range corresponds to the upper limit temperature for

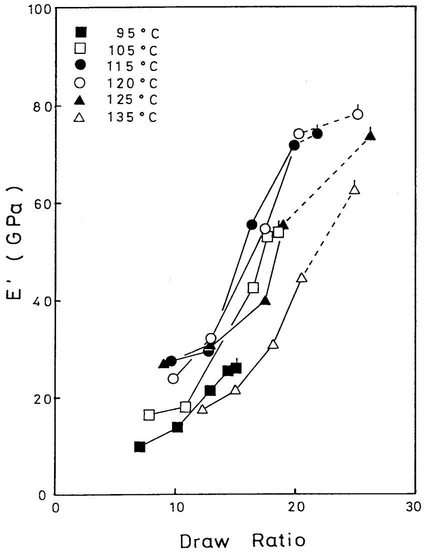

Fig. 3 Young's modulus versus draw ratio for different drawing temperature. The marks with a bar over them are of the multi-stage drawing samples.

crystallite relaxation. Therefore preparing a fiber sample with as high as possible draw ratio in the crystallite relaxation temperature range can be concluded to be the condition for obtaining a high modulus fiber. The sample multi-stage drawn at 120°C attained the young's modulus of 78 GPa with a draw ratio of 25.3.

### 3.3 Structure of zone-drawn fibers

As for the fiber structure developed by zone-drawing, the authors previously proposed a model in which crystallite blocks are interconnected with one another and the oriented amorphous regions are cooped among them. The high amorphous orientation stably maintained even at a room temperature, which is considerably higher than the glass transition point, is attributable to this interconnection among crystallite blocks. With an increase in the interconnection among crystallite blocks the amorphous orientation would conceivably increase. In other words, an increase in the amorphous orientation means a highly developed interconnection among crystallite blocks, and such a fiber structure is thought to effect the high modulus and breaking strength.

Fig. 4 shows crystallinity dependence of amorphous birefringence, which is thought to be related with the interconnection of crystallite blocks. Amorphous birefringence is expressed by two straight lines, one that is drawing temperature independent and another that is drawing temperature dependent with a sharp rise in the dependency at a certain crystallinity, namely a critical point, which tends to shift to the high temperature side with an increase in the drawing temperature.

Fig. 5 shows crystallinity dependence of the young's modulus in a similar manner. As with the case of amorphous birefringence, the relation is expressed by two straight lines. The critical point for the dependency to vary at is found to shift to the high temperature side with an increase in the drawing temperature. The fact that both the amorphous birefringence and the young's modulus are wexpressed each by two straight lines owing to an abrupt change at a certain crystallinity is thought to be related with the increase in the crystallinity and the interconnection of crystallite blocks resulting from drawing. Over a certain crystallinity, the probability for crystallite blocks to interconnect with one another would increase, so that the amorphous molecular chains oriented among crystallite blocks

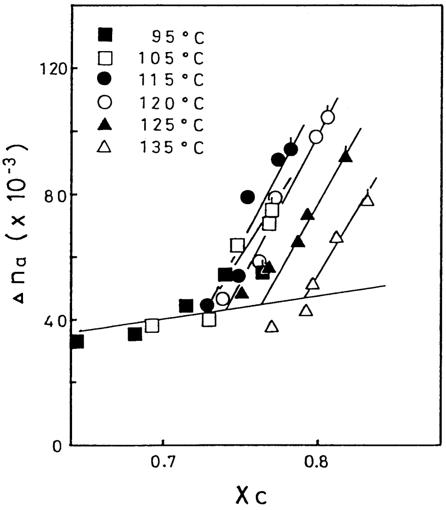

Fig. 4 Amorphous birefringence versus crystallinity for different drawing temperature.

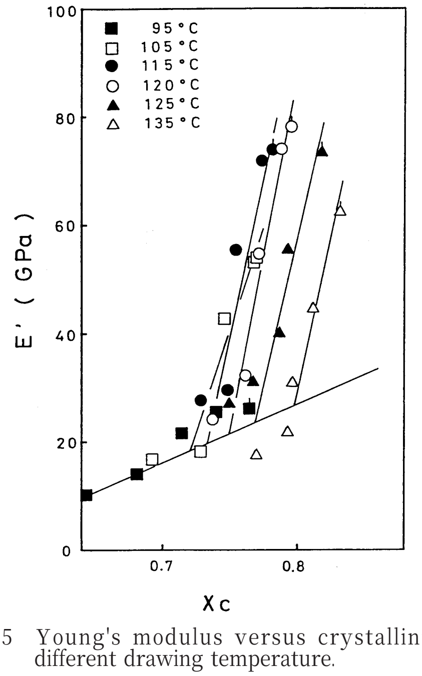

Fig. 5 Young's modulus versus crystallinity for different drawing temperature.

would come to be cooped by the bridging and be less relaxative even at a room temperature higher than the glass transition point. Such a fiber structure is thought to have caused the sharp increase in the modulus.

### 3.4 Thermal shrinkage behavior of zone-drawn fibers

Examination of thermal shrinkage behavior was conducted for: some samples with low modulus because of the low crystallinity positioned below the critical point (at drawing temperature of 95°C); some samples with high modulus because of the high crystallinity positioned above the critical point (at drawing temperature of 120°C); and a sample of gel-drawn UHMWPE. Fig. 6-(a),(b),(c) shows the relationships between the heat treatment temperature and the thermal shrinkage for different drawing temperature. With the samples having the sharply increased modulus due to their position over the critical point, thermal shrinkage was observed to start at a higher temperature than with the samples positioned below the critical point and to be generally small in value. With the gel-drawn sample thermal contraction did not appear up until the melting point.

Thermal shrinkage starting temperature $T_s$, being defined as the temperature for thermal shrinkage to exceed 1%, was plotted against α-relaxation temperature Tα as shown in Fig. 7. With this type of sample, positioned above the critical point and having a high modulus, the thermal contraction initiating temperature Ts appeared in the higher temperature side than Tα. It is therefore understood that with a sample having a high modulus the thermal shrinkage starts in a temperature region higher than the crystallite relaxation temperature. As thermal shrinkage is generally understood to be caused by occurence of amorphous molecular chain relaxation, the result here indicates that the relaxation of amorphous molecular chains oriented to some extent took place after relaxation of crystallites. In other words, at a temperature below Tα the relaxation of the amorphous region is hindered by the crystalline phase, but at a temperature over Tα disruption of the crystallite block linkage caused by the thermal factor is thought to have led to thermal shrinkage. With the gel-drawn sample, on the other hand, its thermal shrinkage starting temperature Ts was by about 30°C higher than Tα, being close to the melting point.

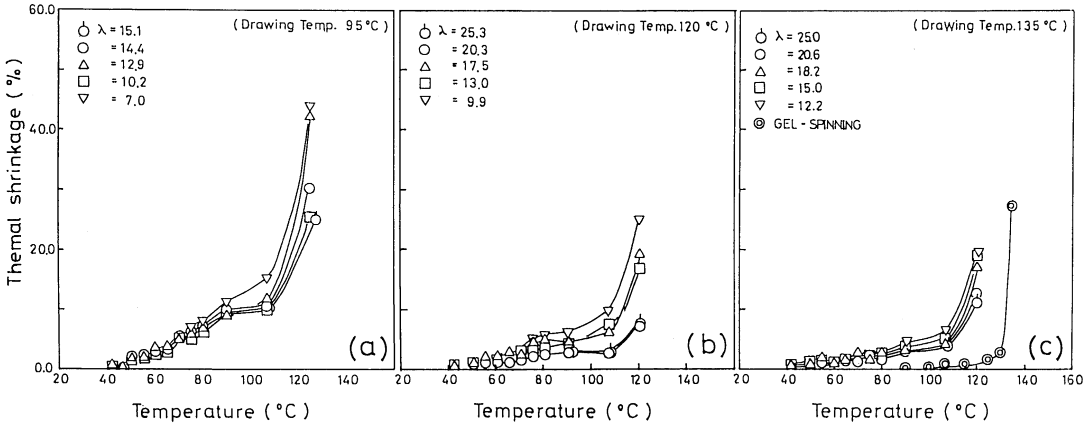

Fig. 6 Thermal shrinkage versus heat treatment temperature for different draw ratio : (a) 95°C of drawing temperature ; (b) 120°C of drawing temperature ; (c) 135°C of drawing temperature.

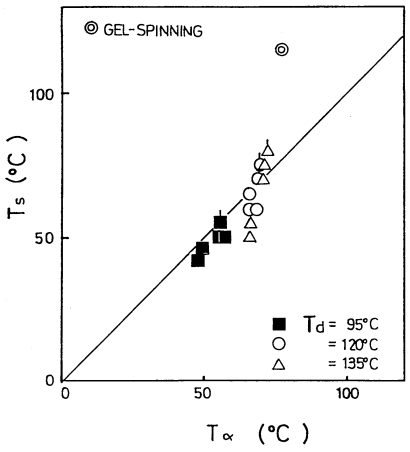

Fig. 7 Relationship between thermal shrinkage starting temperature Ts and α-relaxation temperature Tα.

Fig. 8 shows the relationship between amorphous birefringence and crystallinity for a zone-drawn sample after thermal shrinkage. After a heat treatment (annealing) at 60°C, a temperature below Tα, the amorphous birefringence became lower than that before the heat treatment but still kept a high value. After a heat treatment (annealing) at 70°C, the amorphous birefringence decreased with progress of thermal shrinkage, coming to have a position on the straight line that does not depend on the drawing temperature. When heat treated at 80°C, a temperature above Tα, the sample is found to have been perfectly relaxed. After a heat treatment at 125°C, a temperature close to the melting point, the amorphous birefringence is found to have dropped down to the level of a as-spun fiber, close to the value for non-orientation.

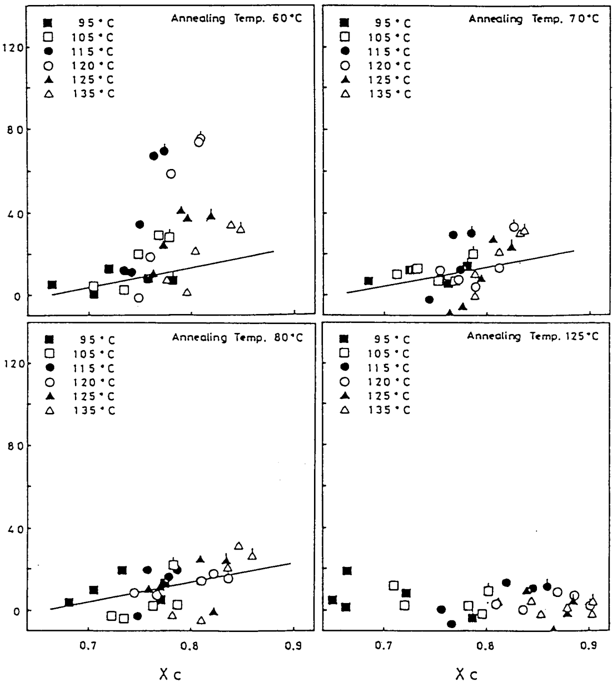

Fig. 8 Amorphous birefringence versus crystallinity after different annealing temperature. The upper left is 60°C of annealing temperature; The upper right is 70°C of annealing temperature; The bottom left is 80°C of annealing temperature; The bottom right is 125°C of annealing temperature.

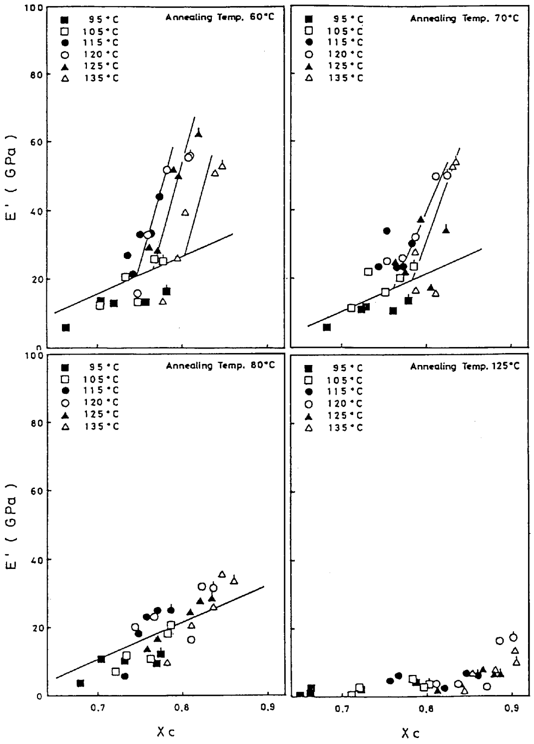

Fig. 9 Young's modulus versus crystallinity after different annealing temperature. The upper left is 60°C of annealing temperature; The upper right is 70°C of annealing temperature; The bottom left is 80°C of annealing temperature; The bottom right is 125°C of annealing temperature.

In a similar manner as above, Fig. 9 shows the relationship between the young's modulus and crystallinity for a zone-drawn sample after thermal shrinkage. After a heat treatment at 60°C, a temperature below Tα, the young's modulus of the sample became somewhat lower than that before the heat treatment but still kept a high value without a marked change. When heat treated at 80°C, a temperature above Tα, the young's modulus of the sample decreased with progress of thermal shrinkage, coming to have a position on the straight line that does not depend on the drawing temperature. After a heat treatment at 125°C, a temperature close to the melting point, the young's modulus dropped down to the level of a as-spun fiber.

At this point, we will consider the model of fiber structure developed by drawing (Fig. 10). (B) and (C) show the sample where young's modulus increased abruptly after the critical point in a continuous zone-drawing and the one before the critical point, respectively. (A) is a sample of a ultra-drawn single crystal of PE having a ultra high molecular weight. Since, in (A) the heat contraction did not start near the melting point of the crystal, a monophasic structure model where defects such as molecular chain ends are distributed randomly is acceptable. On the contrary, for the sample where high mechanical properties were obtained by a continuous zone-drawing of PE having medium to high molecular weights, the heat contraction did not occur until the crystal scattering temperature and high young's modulus were observable. Once the crystalline block is destroyed, a sharp heat contraction occurred and both the amorphous orientation and young's modulus were decreased remarkably. Therefore a model of continuous crystalline blocks such as (B) is conceivable.

On the other hand, the dependence of tensile strength on the crystallinity was shown in Fig. 11. Although the data are scattered considerably, the tensile strength depended on the increase of the crystallinity. When molecular weight increased, it appeared at a higher value on the same crystallinity.

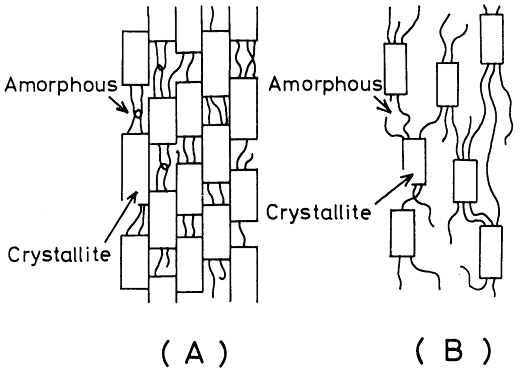

Fig. 10 Schematic representation of fiber structure : (A) intercrystallite bridge model ; (B) conventional crystallite model.

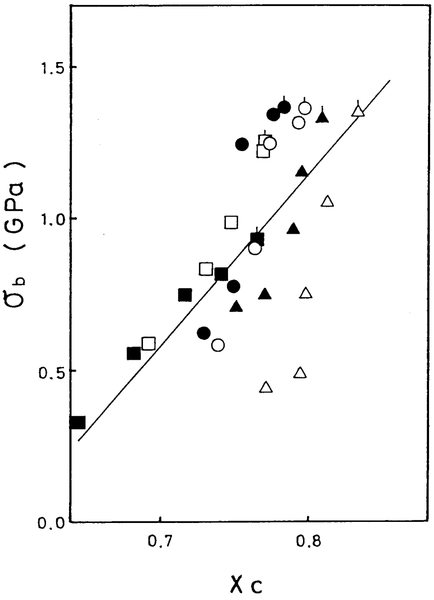

Fig. 11 Tensile strength versus crystallinity for different drawing temperature.

## 4. Conclusions

Structure and properties of high-modulus, high-strength fibers prepared by continuous multi-stage zone-drawing were studied. In particular, thermal properties of the sample including the change in the structure and properties after thermal shrinkage were investigated.

(1) The amorphous birefringence and the young's modulus increased with an increase in draw ratio. With the multi-stage sample, prepared by a necking-drawing followed by a further three-stage non-necking-drawing, both values were positioned on the extrapolating line of the single-stage drawn sample for each drawing temperature.

(2) With a sample having a high crystallinity dependence of the young's modulus and a high modulus, thermal shrinkage started at a higher temperature than with a sample having a low crystallinity dependence of the modulus, generally showing smaller thermal shrinkage. With a gel-drawn sample thermal shrinkage did not occur up until the melting point.

(3) With a sample having a higher crystallinity dependence of the young's modulus, the thermal shrinkage starting temperature Ts appeared at the side of higher temperature than Tα, implying that the thermal shurinkage took place after relaxation of crystallites.

(4) In studies on the structure and properties of a sample after thermal shrinkage, both the young's modulus and the amorphous birefringence maintained high value on heat treating at 60℃, a temperature below Tα, although with some decrease but markedly dropped on heat treating at 80℃, a temperature above Tα.

## References

1) K.Yamaura, M.Suzuki, T.Tanigami1, *Rep. Prog Polym. Phys. Jpn.,* **39**, 209 (1996)
2) H.Van Der Werff, M.H.Hofman, *Chem. fibers int.,* **46**, 435 (1996)
3) H.Fujimatsu, Y.S.Kim, H.Matsuzaki, A.Nakamura, H.Usami, S.Ogasawara, *Polym J.,* **33**, 709 (2001)
4) A.Suzuki, N.Mochiduki, *J. Appl. Polym. Sci.,* **82**, 2775 (2001)
5) N.Okui, M.Takahiro, H.Kikuchi, S.Umemoto, and T.Sakai, *Int. Polym. Proc.,* **1**, 2 (1987)
6) A.Suzuki, M.Ishihara, *J. Appl. Polym. Sci.,* **83**, 1711 (2002)
7) M.Evstatiev, B.Krasteva, S.Fakirov, M.J.Oliveira, T.Serhatkulu, *Int. J. Polym. Mater.,* **50**, 215 (2001)
8) T.Takahashi, T.Tanaka, R.Kamei, N.Okui, M.Takahiro, S.Umemoto, T.Sakai, *Kobunshi Ronbunshu,* **45**, 201 (1988)
9) T.Takahashi, T.Tanaka, R.Kamei, N.Okui, M.Takahiro, S.Umemoto, T.Sakai, *Kobunshi Ronbunshu,* **45**, 209 (1988)
10) T.Takahashi, T.Tanaka, R.Kamei, N.Okui, M.Takahiro, S.Umemoto, T.Sakai, *Sen'i Gakkaishi,* **44**, 165 (1988)
11) T.Takahashi, *Shimane University Bull.,* **36**, 76 (2002)
12) C.R.Desper, J.H.Southern, R.D.Ulrich, and R.S.Porter, *J. Appl. Phys.,* **41**, 4284 (1970)